

Gaps below strange star crusts

Morten Stejner and Jes Madsen

Department of Physics and Astronomy, University of Aarhus, DK-8000 Århus C, Denmark

(Dated: October 31, 2005)

The gap caused by a strong electric field between the quark surface and nuclear crust of a strange star is studied in an improved model including gravity and pressure as well as electrostatic forces. The transition from gap to crust is followed in detail. The properties of the gap are investigated for a wide range of parameters assuming both color-flavor locked and non color-flavor locked strange star cores. The maximally allowed crust density is generally lower than that of neutron drip. Finite temperature is shown to increase the gap width, but the effect is significant only at extreme temperatures. Analytical approximations are derived and shown to provide useful fits to the numerical results.

PACS numbers: 97.60.Jd, 12.38.Mh, 12.39.Ba, 25.75.Nq

I. INTRODUCTION

Strange stars are stars made of absolutely stable quark matter [1, 2, 3, 4]. Their existence (i.e., the stability of strange quark matter) depends on poorly constrained strong interaction properties, and remains to be decided by observation or experiment (see [5, 6] for reviews). If strange stars are stable, they contain roughly equal numbers of up, down, and strange quarks, but due to the higher mass of the s-quark, they will normally contain a slight deficit of strange quarks with negative charge, and thus have an overall positive quark charge to be compensated by electrons. Even color-flavor locked quark matter, which is electrically neutral in bulk [7], has an overall positive quark charge due to surface effects [8, 9, 10]. The quark surface of a strange star is very sharp (the density drops from above nuclear matter density to zero within a few fm), and since the electrostatic force is weaker than the strong force, some of the electrons necessary to create an overall charge neutral object will form a thin atmosphere with a huge electric field (up to 10^{18} V/cm) outside the quark phase. This field is capable of sustaining a nuclear matter crust decoupled from the quark phase by an electron-filled gap. The maximum mass of such a crust is approximately $2 \times 10^{-5} M_{\odot}$, corresponding to the situation where the inner boundary of the crust reaches the neutron drip density, 4×10^{11} g cm $^{-3}$, where neutrons drip out of crust nuclei and get dissolved in the quark phase. Smaller crust mass limits would occur if the gap is sufficiently narrow to allow direct contact with the crust or if the rate of quantum tunneling of nuclei into the quark core of the star is large. The crust mass and moment of inertia as well as the coupling between core and crust play important roles in the understanding of strange star properties, and therefore the properties of the gap are very important. The width of this gap is the main topic of the present investigation.

The properties of the electron atmosphere and the impact on a nuclear matter crust have been studied by many authors, including [4, 10, 11, 12, 13, 14, 15, 16, 17]. These studies have involved solutions to the Poisson equation

for the electrostatic potential with the boundary condition of electric neutrality deep within the strange star, as well as a condition for the potential at large distances. For bare strange stars, i.e., stars without a nuclear crust, the potential goes to zero at infinity. For strange stars accreting nuclear matter on the surface, the condition has been taken to be a matching of the electric potential from the electrons to the value of the potential required in the bulk of the nuclear matter crust (typically several MeV, depending on the crust density). This leads to a typical gap size (distance from quark surface to the inner surface of the nuclear crust) of $10^2 - 10^3$ fm, comparable to the distance over which the potential drops by a factor of a few.

The approaches just described do not account however for the detailed balance between electrical and gravitational forces and pressure in the transition from gap to crust. The potential and its derivative are taken to be continuous across the crust boundary while gravitational forces and pressure in the crust are assumed insignificant (though see [12] for an approximate inclusion of gravity). In this work we expand earlier treatments, investigate the effects of including the Newtonian gravitational field, and find the detailed structure of the gap and the transition to the crust. This leads to more narrow gaps than previously found and thus constrains the density at the base of the crust below the neutron drip density. As the temperature increases, the additional thermal reservoir of electrons initially widens the gap then narrows it, but even for temperatures as high as 10^7 K in the gap region this effect is small and the width remains constant up to temperatures in the range $10^8 - 10^{10}$ K depending on the crust density.

II. EQUILIBRIUM OF THE CRUST

The effective chemical potential of species i , μ_i^{eff} , is defined as the change in energy for a unit change in number density of species i , while the volume, entropy, and other number densities are kept constant. In a steady state as-

suming the crust to be isothermal the effective chemical potentials of electrons and nuclei should be constant to avoid migration. They must therefore be equal to their values at the top of the crust, at radius $r = R$, where the electric potential is zero and the chemical potentials are equal to the particle masses. Therefore we take the effective chemical potentials for electrons and nuclei to be

$$\begin{aligned}\mu_e^{\text{eff}} &= \mu_e(r) - e\phi_e(r) + m_e\phi_g(r) = m_e + m_e\phi_g(R) \\ \mu_e(r) &= m_e + m_e[\phi_g(R) - \phi_g(r)] + e\phi_e(r) \\ \mu_N^{\text{eff}} &= \mu_N(r) + Ze\phi_e(r) + m_N\phi_g(r) = m_N + m_N\phi_g(R) \\ \mu_N(r) &= m_N + m_N[\phi_g(R) - \phi_g(r)] - Ze\phi_e(r).\end{aligned}\quad (1)$$

For simplicity we describe electrons as well as nuclei as Fermi gases characterized by thermodynamic chemical potentials μ_e and μ_N . m_e is the electron mass, m_N is the mass of the dominant nucleus at the base of the crust, Z is its charge, $\phi_e(r)$ is the electric potential and $\phi_g(r)$ is the gravitational potential for which we will use the Newtonian value to get tractable expressions. $e\phi_e$ is typically of the order of 20 MeV at the strange core surface, $r = R_S$, and $\phi_g(R_S) = -GM_S/R_S \sim -0.2$, where M_S is the mass of the strange core.

We note at this point that keeping the effective chemical potentials constant corresponds to hydrostatic equilibrium which may be seen explicitly by taking the gradient of the above expressions and using the zero temperature identity $dP_i = n_i d\mu_i$, where P_i is the pressure and n_i the number density of the i 'th component.

$$\begin{aligned}\frac{dP_e}{dr} - n_e \frac{d(e\phi_e)}{dr} + n_e m_e \frac{d\phi_g}{dr} &= 0 \\ \frac{dP_N}{dr} + Zn_N \frac{d(e\phi_e)}{dr} + n_N m_N \frac{d\phi_g}{dr} &= 0\end{aligned}$$

The total pressure is $P = P_e + P_N$ so the sum then gives the usual force balance

$$\frac{dP}{dr} + n_q \frac{d(e\phi_e)}{dr} + \rho \frac{d\phi_g}{dr} = 0 \quad (2)$$

with $n_q = Zn_N - n_e$ the charge density and $\rho = m_e n_e + m_N n_N$ the mass density. We show later that Eq. (2) is convenient when approximating thin crusts.

To solve for the chemical potentials we take the Laplacian of Eq. (1) and use Poisson's equation in Newtonian gravity to get a system of coupled differential equations in the chemical potentials and their derivatives. With the understanding that the core at $r < R_S$ is comprised of quarks and electrons while only electrons are present in the gap at $R_S < r < R_C$, and that nuclei do not appear until $\mu_N > m_N$ at $r > R_C$ this gives in a compact

notation

$$\begin{aligned}\nabla^2 \mu_e(r) &= \frac{d^2 \mu_e}{dr^2} + \frac{2}{r} \frac{d\mu_e}{dr} \\ &= \nabla^2 [e\phi_e(r) - m_e\phi_g(r)] \\ &= -4\pi e^2 (n_q^+ + Zn_N - n_e) \\ &\quad - 4\pi G m_e (\rho_q + m_N n_N + m_e n_e)\end{aligned}\quad (3)$$

$$\begin{aligned}\nabla^2 \mu_N(r) &= \frac{d^2 \mu_N}{dr^2} + \frac{2}{r} \frac{d\mu_N}{dr} \\ &= \nabla^2 [-Ze\phi_e(r) - m_N\phi_g(r)] \\ &= 4\pi e^2 Z (n_q^+ + Zn_N - n_e) \\ &\quad - 4\pi G m_N (\rho_q + m_N n_N + m_e n_e)\end{aligned}\quad (4)$$

Here ρ_q is the approximately constant mass density of the quark matter and n_q^+ is its positive charge density – we assume that the quark distribution is not significantly affected by the crust (see however the recent work by Jaikumar et al. [16]). In these equations we have used rest mass times number density for the matter density in Poissons equation. This is a very rough approximation for the electrons as they are relativistic except for very thin crusts, but in all the calculations below we will neglect the electron contribution to the density completely by taking $m_e = 0$. The densities of electrons and nuclei are found from

$$n_i = \int d^3 p_i \frac{g_i}{h^3} f(p_i), \quad f(p_i) = \frac{1}{e^{(E_i - \mu_i)/T} + 1} \quad (5)$$

where p is the particle momentum, g_i the statistical weight, $E_i = \sqrt{p_i^2 + m_i^2}$ the energy and $f(p)$ the Fermi-Dirac distribution. For a cold Fermi gas with $g_i = 2$ this gives

$$n_i = \frac{(\mu_i^2 - m_i^2)^{3/2}}{3\pi^2}. \quad (6)$$

while for finite temperatures there will be additional thermal electrons and working in the approximation $m_e = 0$ the net electron density (electrons minus positrons) will be

$$n_e = \frac{\mu_e^3}{3\pi^2} + \frac{\mu_e T^2}{3} \quad (7)$$

Equations (3) and (4) can thus be transformed into four first order coupled differential equations in the four unknowns $\mu_e, \mu_N, \frac{d\mu_e}{dr}, \frac{d\mu_N}{dr}$. Given appropriate boundary conditions at some point – usually either in the charge neutral bulk of the strange star core or at the core surface – the system can be solved to find the structure of the gap and the transition to the crust. In principle we could extend the model to include the entire crust, but it should be noted that we have not included the interactions between nuclei (apart from the mean electric potential and gravity) and that the global properties of the crust should be described using relativistic gravity and a more advanced equation of state – such as the BPS

equation of state. Here we restrict ourselves to modeling the gap and the lower crust until the point where charge neutrality is achieved. The density at this point can then be taken as the inner crust density used to parametrize the crust models in e.g. [17].

III. APPROXIMATIVE MODELS

Before we get into the detailed numerical models it is worth noticing that a number of illustrative approximate models can be calculated analytically, and that as it turns out these models reproduce the behavior of the system accurately.

First of all it should be noted that we can get a very useful relation from Eq. (1) by taking the sum

$$\mu_N(r) + Z\mu_e(r) = (m_N + Zm_e)[1 + \phi_g(R) - \phi_g(r)] \quad (8)$$

and its derivative

$$\frac{d\mu_N(r)}{dr} + Z\frac{d\mu_e(r)}{dr} = -(m_N + Zm_e)\frac{d\phi_g(r)}{dr}. \quad (9)$$

From this and equations (3, 4) we can get a qualitative idea of the form of the solutions. For example we know that just above the strange core surface the electric potential should be large and positive and its gradient should be large and negative while the gravitational potential and its gradient can be approximated by their Newtonian values. Only electrons are present at this point so the charge density is negative, and μ_e will be large and decreasing rapidly but with a positive curvature. Since the right hand side of equation (8) is almost constant across the gap μ_N must increase as μ_e decreases. Thus we also see that μ_e must decrease monotonically since μ_e and μ_N would diverge in opposite directions if μ_e started increasing while the charge density was still negative and $\mu_e(r)$ was curving upwards. Once $\mu_N > m_N$ we enter the crust and at some point achieve charge neutrality. $\mu_N(r)$ curves downwards only if the charge density is negative and since we expect the crust to be charge neutral in bulk μ_N must start decreasing along with μ_e at this point for the crust to remain charge neutral. The right hand side of equation (9) is of the order of $\sim -10^{-15}$ MeV/fm so for both $\frac{d\mu_e}{dr}$ and $\frac{d\mu_N}{dr}$ to be negative they must both be numerically smaller than 10^{-15} MeV/fm. Since $\frac{d\mu_e}{dr}$ will generally be of the order of 0.1 MeV/fm close to the surface of the strange star core this places high demands on the numerical procedure as it must be accurate across these many orders of magnitude. This difficulty stems from the fact that we are trying to model the transition from the gap where the strong electrical force is dominant to a charge neutral crust held down by the much weaker gravitational force – a very stiff set of equations.

To get something more quantitative than these heuristic arguments we will use the approximation $m_e = 0$.

This allows us to solve for μ_e in the case of a pure electron atmosphere with no crust. This can then be used to find approximate expressions for the gap width. For more realistic solutions it should be taken into account that some of the electrons from the crust will spill into the gap shielding the strange star core surface charge and affecting the gap width. We study the full solutions numerically in a later section, but these are much easier to understand (and find) with the insight from the qualitative models below.

A. The pure electron atmosphere around a bare strange star

For a pure electron atmosphere with $m_e = 0$ we have $\mu_e(r) = e\phi_e(r)$ and in general

$$n_e = \frac{(e\phi_e)^3}{3\pi^2} + \frac{(e\phi_e)T^2}{3}. \quad (10)$$

Following [14, 15] we define $y = d(e\phi_e)/dz$ where z is the height above the strange core surface. Assuming a flat strange core surface Eq. (3) then takes the form

$$\frac{d(y^2)}{d(e\phi_e)} = 4C^{-2}((e\phi_e)^3 + \pi^2T^2(e\phi_e)) \quad (11)$$

where $C = \sqrt{3\pi/2}/e = 5013$ MeV fm. This may be solved directly for the electric field and potential using the fact that both should go to zero at large z :

$$-\frac{d(e\phi_e)}{dz} = C^{-1}((e\phi_e)^4 + 2\pi^2T^2(e\phi_e))^{1/2} \quad (12)$$

$$z = \frac{C}{\sqrt{2}\pi T} \left[\sinh^{-1} \left(\frac{\sqrt{2}\pi T}{e\phi_e(r)} \right) - \sinh^{-1} \left(\frac{\sqrt{2}\pi T}{e\phi_e(R_S)} \right) \right] \quad (13)$$

where we give $z(e\phi)$ as this is what we will need later. It may be noted that in the limit $T \rightarrow 0$ equation (13) reduces to the expression found by Alcock et al. in [4] since $\sinh^{-1} x \sim x$ for $x \rightarrow 0$

$$e\phi_e(r) = \frac{C}{z + C/e\phi_e(R_S)} \text{ for } T = 0. \quad (14)$$

A plot of this behavior can be found in Fig. 1. Note that we have included the case $e\phi_e(R_S) = 30$ MeV. In the models below this just allows a crust at neutron drip density to remain out of direct contact with the strange core surface making it an illustrative case, though the choice is difficult to realize for non color-flavor locked quark matter equations of state [18].

B. Thin crusts and test particles

Sufficiently thin crusts should not be expected to change the electric potential or the distribution of electrons in the gap from that of a pure electron atmosphere.

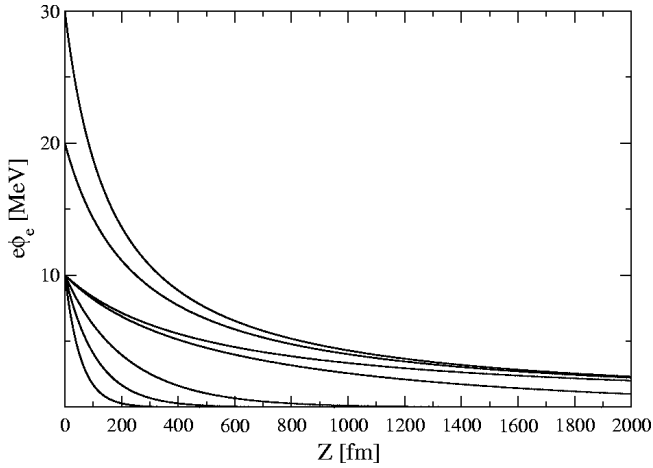


FIG. 1: Electric potential above the surface of a bare strange star. From the top $e\phi_e(R_S) = 30, 20, 10$ MeV. We show the variation with temperature for $e\phi_e(R_S) = 10$ MeV so from the top $T = 0, 1, 5, 10, 20$ MeV for these.

We can then use the solution found in the previous subsection and demand that equation (2) is obeyed at the crust boundary. Since we are working in the approximation $m_e = 0$ the electronic part of the force balance is simply $\frac{dP_e}{dr} - n_e \frac{d(e\phi_e)}{dr} = 0$ which is trivially fulfilled since $\mu_e = e\phi_e$ and $dP_e = n_e d\mu_e$. For a thin crust we should be able to ignore the pressure gradient from the nuclei and the remainder of the force balance equation involves only the equilibrium between electrostatic repulsion and gravitational attraction of positively charged nuclei:

$$Zn_N \frac{d(e\phi_e)}{dr} + \frac{GM_S n_N m_N}{r^2} = 0 \quad (15)$$

The number density of nuclei then cancels and the equation simply expresses that each individual nucleus feels a balance between the gravitational attraction from the strange star core and the electrostatic repulsion from the net positive charge below it as described by $d(e\phi_e)/dr$. This is the same equation as would be obtained by balancing a single positively charged test particle above the strange star surface. In the case of a cold atmosphere we use the derivative of equation (14) for the electric field which leads to the relation

$$-\frac{C}{(z_{gap} + C/e\phi_e(R_S))^2} = -\frac{GM_S m_N}{ZR_C^2}, \quad (16)$$

or $z_{gap} \equiv R_C - R_S \simeq R_S(CZ/GM_S m_N)^{1/2} \simeq 10^{10}$ fm. The gap width of very thin crusts is therefore almost macroscopic in size as might be expected since the lower layer does not have to support the bulk of the crust. If we assume that equation (15) is obeyed identically throughout the entire crust as it should be if the pressure gradient from the nuclei remains negligible we can solve for the potential

$$e\phi_e(r > R_C) = \frac{GMm_N}{Zr} + K, \quad (17)$$

where K is a constant. This potential is a solution to Poisson's equation without a source term,

$$\nabla^2(e\phi_e) = \frac{d^2(e\phi_e)}{dr^2} + \frac{2}{r} \frac{d(e\phi_e)}{dr} = 0 \quad (18)$$

showing that the crust is locally charge neutral in this approximation.

C. Cold charge neutral crusts

In heavy dense crusts the pressure from the nuclei can not be ignored, and we would need the precise density profile to solve equation (2). The crust would still be expected to be charge neutral beyond some point not very far from the crust boundary however, so by assuming charge neutrality and using equation (8) it is possible to estimate μ_e at the crust boundary. The gap width can then be found assuming that the potential in the gap can be described by the solution for a pure electron atmosphere.

For a cold crust charge neutrality in the Fermi gas approximation is described by the requirement

$$\frac{(\mu_e^2 - m_e^2)^{3/2}}{3\pi^2} = Z \frac{(\mu_N^2 - m_N^2)^{3/2}}{3\pi^2}. \quad (19)$$

Solving for μ_e and using relation (8) this gives

$$\begin{aligned} \mu_e = & \left((m_N + Zm_e)[1 + \phi_g(R) - \phi_g(r)] - \right. \\ & \left[(m_N^2 - Z^{-2/3}m_e^2)(1 - Z^{-8/3}) + \right. \\ & \left. Z^{-8/3}[(m_N + Zm_e) \right. \\ & \left. (1 + \phi_g(R) - \phi_g(r))]^2 \right]^{1/2} \left. \right) (Z(1 - Z^{-8/3}))^{-1}. \end{aligned} \quad (20)$$

Taking $m_e = 0$ and using $\phi_g(R) - \phi_g(r) \ll 1$ this simplifies to

$$\begin{aligned} \mu_e = & \frac{m_N}{Z} \left[(\phi_g(R) - \phi_g(r)) \right. \\ & \left. - \frac{1}{2}(Z^{8/3} - 1)[\phi_g(R) - \phi_g(r)]^2 \right]. \end{aligned} \quad (21)$$

Using equation (8) again and $\rho = n_N m_N$ this leads to a relation between the size, mass, density and composition of the crust

$$\phi_g(R) - \phi_g(r) = \left[2 \frac{\mu_N - m_N}{m_N} (Z^{8/3} - 1) \right]^{1/2} \quad (22)$$

$$= 1.9 \times 10^{-4} \left(\frac{\rho}{\rho_D} \right)^{1/3} \left(\frac{56}{A} \right)^{4/3} (Z^{8/3} - 1)^{1/2}, \quad (23)$$

where $\rho_D = 4 \times 10^{11}$ g/cm³ is the neutron drip density. Assuming that charge neutrality occurs shortly after the crust boundary at R_C , $\phi_g(r)$ will not change

much between these two points and we can use this to estimate $\mu_e(R_C)$. The crust boundary is defined by $\mu_N = m_N$ and from equation (8) we then have $\mu_e(R_C) = \frac{m_N}{Z}(\phi_g(R) - \phi_g(R_C))$ which can be used with the potential (14) to find the gap width

$$\begin{aligned} z_{gap} &= \frac{C}{\mu_e(R_C)} - \frac{C}{e\phi_e(R_S)} \\ &= 505 \left(\frac{\rho}{\rho_D}\right)^{-1/3} \left(\frac{A}{56}\right)^{1/3} Z(Z^{8/3} - 1)^{-1/2} \text{ fm} \\ &\quad - \frac{167 \text{ fm}}{e\phi_e(R_S)/30\text{MeV}} \\ &= 170.5 \left(\frac{\rho}{\rho_D}\right)^{-1/3} \text{ fm} - 167 \left(\frac{e\phi_e(R_S)}{30 \text{ MeV}}\right)^{-1} \text{ fm}. \end{aligned} \quad (24)$$

The last equality assumes a crust composed of electrons and ^{56}Fe nuclei. In this approximation the gap width is very small near neutron drip density, and for a realistic value of $e\phi_e(R_S) \sim 20$ MeV it would be impossible for a crust to reach neutron drip density while remaining out of contact with the strange star core. If the more stringent limit of $z_{gap} > 200$ fm from [4] for the crust to remain secure against strong interactions with the strange star core is used, the maximum crust density is $\sim 0.1\rho_D$. We will see later that this simple relation describes the outcome of the numerical calculations very well.

D. Charge neutral crust at finite temperatures

At finite temperatures the electron density is given by equation (7), and we will approximate the electric potential in the gap by equation (13). As before the crust boundary is given by $\mu_N(R_C) = m_N$ so $\mu_e(R_C) = e\phi_e = \frac{m_N}{Z}\Delta\phi_g$ by equation (8) with $\Delta\phi_g = \phi_g(R) - \phi_g(R_C)$, and we will again assume that charge neutrality occurs shortly after the crust boundary so we can solve $n_e = Zn_N$ for $\Delta\phi_g$. Because of the extra electrons this can not be done analytically since the equation for $\Delta\phi_g$ now becomes

$$\begin{aligned} 0 &= Z(\mu_N^2 - m_N^2)^{3/2} - (m_N[1 + \Delta\phi_g] - \mu_N)^3 Z^{-3} \\ &\quad - 3\pi^2(m_N[1 + \Delta\phi_g] - \mu_N)T^2/3Z \end{aligned} \quad (25)$$

with

$$\mu_N = ((3\pi^3\rho/m_N)^{2/3} + m_N^2)^{1/2}. \quad (26)$$

These equations can however be solved numerically for $\Delta\phi_g(\rho, T)$ which gives $\mu_e(R_C)$ and z_{gap} as shown in Fig. 6. Qualitatively we note that changes from the cold case are negligible until temperatures around 1 MeV or 10^{10} K are reached – that is until the temperature is comparable to μ_e in the bulk of the crust. For lower densities the effect occurs at somewhat lower temperatures, but by then the gap is already very large and the temperature

does not really change this. The bump in the gap size seen at high temperatures can be understood from equations (13) and (25). The temperature dependent part of equation (25) shows that $\Delta\phi_g$ and thus $e\phi_e(R_C)$ will be constant for low temperatures, $T \ll \mu_e$ ($r \gg R_C$), and smaller for higher temperatures. Since $\sinh^{-1} x \sim x$ for $|x| < 1$ and $\sinh^{-1} x \sim \log 2x$ for $x > 1$ this can produce the bump. Physically the thermal electrons in the crust means that μ_e does not have to be as large to reach a certain density, which moves the crust boundary further out, while the thermal electrons in the gap screens the strange star surface charge and reduces the gap.

IV. NUMERICAL SOLUTIONS

A. Numerical procedure and boundary conditions

To solve equations (3) and (4) numerically we employ a shooting method which integrates the equations from the quark core to the point of charge neutrality in the crust using a standard Runge-Kutta routine. We then vary $d\mu_e/dr$ at the starting point until equation (9) is fulfilled at charge neutrality so the crust remains charge neutral beyond this point. Equations (1) would seem to produce many more free parameters at the starting point than just $d\mu_e/dr$, but since $e\phi_e(r)$ at the quark core depends on unknown details of the quark matter equation of state we keep it free and explore the solutions for a wide range of this parameter. Furthermore it was shown in the preceding sections that the quantity $\Delta\phi_g = \phi_g(R) - \phi_g(R_C)$ is related to the density of the crust in the charge neutral bulk through equations (23) and (25) – and as it turns out these relations are fulfilled for the numerical solutions as well. Since $d\mu_N/dr$ may be determined at the starting point by equation (9) this leaves $d\mu_e/dr$ as the only parameter to be determined. With this method we can thus choose $e\phi_e(r)$ at the starting point (this corresponds to choosing parameters for the equation of state for the strange matter core) and a crust – described by its density ($\Delta\phi_g$) and temperature at charge neutrality – and find the solution to equations (3) and (4) describing the transition between the core and crust.

We have so far not specified the exact location of the starting point for the integration because the discussion above does not depend on this, and because the assumption of a color-flavor locked quark core places the starting point at the core surface, whereas for a non color-flavor locked core it should be taken in the charge neutral bulk of the core. Color-flavor locked strange quark matter is charge neutral in bulk because the pairing minimizes the energy for equal quark Fermi momenta leading to equal numbers of u-, d-, and s-quarks. However as discussed in [9] when surface effects are taken into account there will be a deficit of s-quarks near the surface producing an overall positive surface charge. As shown in [10] this gives a Coulomb barrier at the surface of the order of $e\phi_e(R_s) \sim 36$ MeV. For color-flavor locked stars we thus

take the starting point at the surface of the quark core and find solutions for different values of $e\phi_e(R_s)$ and different crusts.

In non color-flavor locked stars the deficit of s-quarks is global and compensated by electrons in the bulk. The surface charge here arises because some electrons near the surface leave the core and create an atmosphere outside the quark phase. We therefore take the starting point “deep” in the core (1000 fm below the surface; our results are insensitive to this choice) where we assume charge neutrality, $n_q^+(\mu_q^+) = n_e(\mu_e, T)$,

$$\frac{\mu_q^{+3}}{3\pi^2} = \frac{\mu_e^3}{3\pi^2} + \frac{\mu_e T^2}{3}. \quad (27)$$

The chemical potential for the quark charge, μ_q^+ , defined by this relation, was explored in eg. [4, 11, 18] and found to be of the order of $\mu_q^+ \simeq 25$ MeV. However the same surface effect which gives rise to the strange quark deficit in color-flavor locked stars will reduce the number of strange quarks further. We do not explicitly include this effect in our calculations.

B. Chemical composition of the crust

The chemical composition of the crust depends on its origin and the accretion history of the strange star. If the crust was created in the supernova along with the strange star and has not changed since, it will consist of cold catalyzed matter as described by the BPS equation of state in [19]. If the crust was accreted from a companion star temperatures do not become high enough for the matter to reach the equilibrium described by the BPS equation of state. Instead hydrogen is burned at the surface to helium which is in turn burned explosively in X-ray bursts and leaves a layer of heavy ashes at densities exceeding 10^8 g/cm³. The ashes then sink under the weight of accreted matter and under the increasing pressure its composition changes in a series of electron captures until neutron drip sets in. This process has been investigated by Haensel & Zdunik, and the chemical composition as a function of density was given in [20], assuming that the ashes left by the X-ray bursts are composed of ⁵⁶Fe. The composition of the X-ray burst ashes is a matter of some debate however, and as it was shown by Schatz et al. in [21] that *rp*-processes in the X-ray bursts may lead to a composition dominated by much heavier nuclei with $A \sim 106$, Haensel & Zdunik recently revised the resulting chemical composition in [22]. However it was also suggested by Schatz et al. [23] that the X-ray burst ashes may burn explosively at densities around $\sim 10^9$ g/cm³ powering X-ray superbursts in which case photodisintegration will lead to a composition similar to that found in [20].

For our purpose we chose the relevant nucleus from these articles based on the density in the crust at the point of charge neutrality – the transition from gap to

crust takes place over just a few fm so there is no reason to assume any other nucleus will play a role. As discussed the actual composition is rather uncertain, so we include calculations for each of the three scenarios. The charge to mass ratios are very similar, so the only significant difference turns out to be related to the different values for the neutron drip density. The chemical compositions used are shown at densities below neutron drip in Table I. We hereafter refer to the compositions in [19, 20, 22] as BPS, HZ1990 and HZ2003 respectively. For the HZ1990 and HZ2003 compositions which arise from explosive helium burning we assume a composition of pure ⁴He below 10^8 g/cm³. This transition should be more smooth, but it hardly matters as the gap width is already very large at these densities and small corrections from the composition will not affect this.

Ref. [19] – BPS		Ref. [20] – HZ1990		Ref. [22] – HZ2003	
ρ_{max} [g/cm ³]	Nucleus	ρ_{max} [g/cm ³]	Nucleus	ρ_{max} [g/cm ³]	Nucleus
8.1×10^6	⁵⁶ Fe	1.494×10^9	⁵⁶ Fe	3.517×10^8	¹⁰⁶ Pd
2.7×10^8	⁶² Ni	1.115×10^{10}	⁵⁶ Cr	5.621×10^9	¹⁰⁶ Ru
1.2×10^9	⁶⁴ Ni	7.848×10^{10}	⁵⁶ Ti	2.413×10^{10}	¹⁰⁶ Mo
8.2×10^9	⁸⁴ Se	2.496×10^{11}	⁵⁶ Ca	6.639×10^{10}	¹⁰⁶ Zr
2.2×10^{10}	⁸² Ge	6.110×10^{11}	⁵⁶ Ar	1.455×10^{11}	¹⁰⁶ Sr
4.8×10^{10}	⁸⁰ Zn			2.774×10^{11}	¹⁰⁶ Kr
1.6×10^{11}	⁷⁸ Ni			4.811×10^{11}	¹⁰⁶ Se
1.8×10^{11}	⁷⁶ Fe			7.785×10^{11}	¹⁰⁶ Ge
1.9×10^{11}	¹²⁴ Mo				
2.7×10^{11}	¹²² Zr				
3.7×10^{11}	¹²⁰ Sr				
4.3×10^{11}	¹¹⁸ Kr				

TABLE I: Chemical composition of the crust as a function of density for the three scenarios discussed in the text. ρ_{max} is the maximum density at which a nucleus is present before it undergoes electron capture.

V. RESULTS FOR COLOR-FLAVOR LOCKED STRANGE STAR CORES

We have found solutions for a range of densities, compositions and temperatures of the crust as well as for different electric potentials at the quark core surface. The basic features of one such solution with $\rho_{crust} = 4 \times 10^{11}$ g/cm³, $T = 0$, $e\phi(R_s) = 30$ MeV and the crust composition in HZ2003 are shown in Figs. 2, 3, and 4. The numerical solution conforms with the general behavior discussed previously, but it should be noted that the actual transition to the crust takes place over less than a fm; smaller than the radius of the relevant nuclei. A model based on statistical physics should hardly be trusted on such scales and the most reasonable conclusion would probably be that the density is essentially discontinuous at the crust boundary.

The dependence of the gap width on density, composition and electric potential at the quark surface is explored

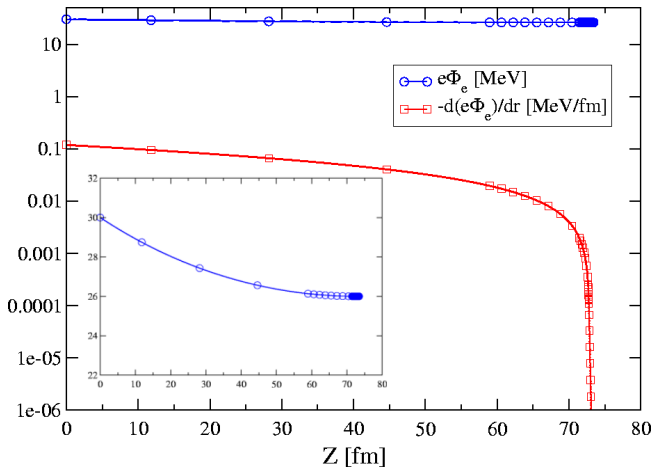


FIG. 2: Electric potential and field for a typical solution. Note how the field dies out in the charge neutral bulk of the crust. The inset focuses on the electric potential.

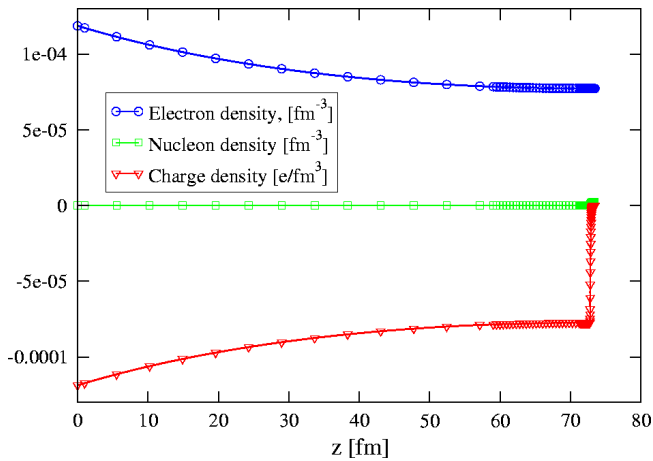


FIG. 3: Electron, nucleon and charge density for the solution in Fig. 2. The transition to the crust is shown in Fig. 4.

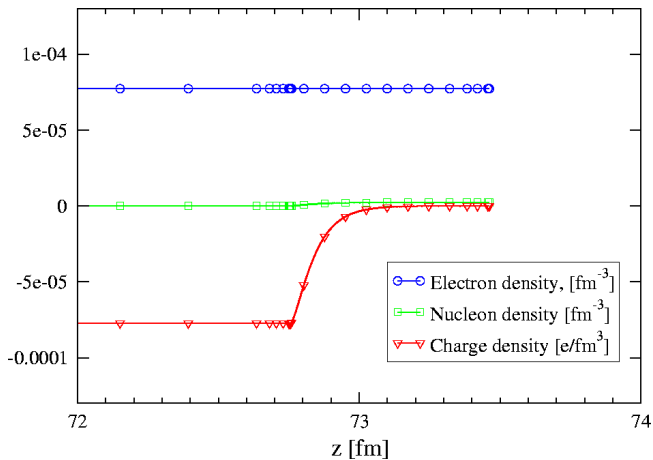


FIG. 4: Electron, nucleon and charge density during the transition to the crust for the solution in Figs. 2 and 3. Nucleons appear over a few fm and charge neutrality is attained in the crust.

at zero temperature in Fig. 5 and compared to the analytical approximation in Eq. (24). In each case we plot (close) to the highest possible density, which is either the neutron drip density given in Table I or the density at which $z_{\text{gap}} \sim 0$. The gap width is insensitive to the choice of chemical composition, but it may be noted that only for high $e\phi_e(R_s)$ is it possible to reach neutron drip density before the gap width goes to zero. In particular the BPS and HZ1990 compositions are limited by neutron drip at $e\phi_e(R_s) = 30$ MeV whereas the gap width goes to zero before neutron drip for the HZ2003 composition. As noted previously this choice of $e\phi_e(R_s)$ is therefore quite illustrative and we will often use it below.

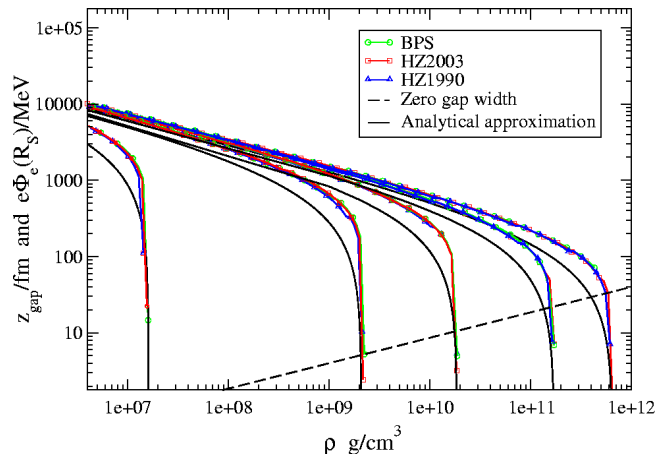


FIG. 5: Gap width dependence on density, crust composition and electric potential at the quark surface for color-flavor locked cores. From left to right $e\phi_e(R_s)$ is 1, 5, 10, 20 and 30 MeV. Curves for different composition are almost indistinguishable. The analytical approximations are based on Eq. (24) using the crust composition from the BPS equation of state. The dashed line shows the solution of Eq. (24) with $z_{\text{gap}} = 0$ – i.e. the density at which the gap width goes to zero for a specific $e\phi_e(R_s)$.

Figure 6 shows the temperature dependence of z_{gap} with $e\phi_e(R_s) = 30$ MeV. Temperatures up to 100 MeV are shown to illustrate the full range of solutions, but one should keep in mind that the Coulomb barrier is only 30 MeV or less, and so can not hold the nuclei at these temperatures. $e\phi_e(R_s)$ is set very high to allow high densities, and for simplicity we only vary the composition for the maximum density curves discussed above. We recover the qualitative features of the analytical approximation. Except perhaps for the very early stages after formation in a supernova explosion crust temperatures of isolated strange stars are expected to be much smaller than 0.1 – 1 MeV where the temperature effects for the gap width become noticeable. Interesting temperatures may be reached in accreting binary systems to which we return in a later section. It may also be relevant that the increase in gap width allows a strange star to sustain a crust shortly after its formation in the supernova

even when temperatures are very high – whether a crust would actually form at that stage is a different matter.

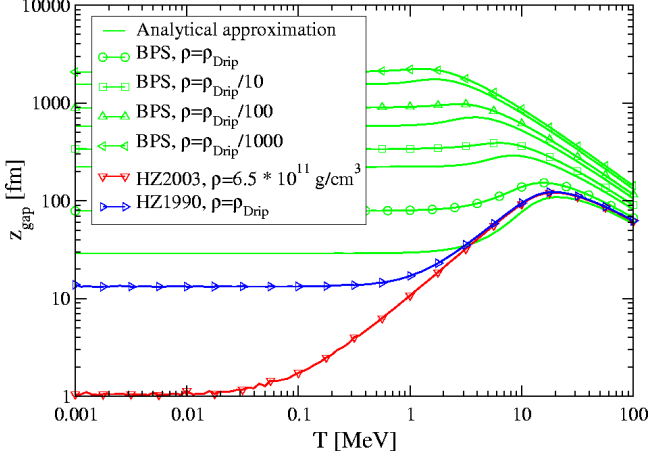


FIG. 6: Gap width dependence on temperature, density and crust composition for color-flavor locked cores with $e\phi_e(R_S) = 30$ MeV. Densities increase from top to bottom and curves without points show analytical approximations based on Eq. (25). For simplicity we only vary the composition for the maximum density crusts. The HZ2003 curve has a very low gap width because its density is not limited by neutron drip.

Perhaps a better measure of the stability of the crust is the transmission coefficient for ions through the gap, τ , which following Alcock et al. [4], can be found in the WKB approximation by

$$\tau = \exp \left[-2 \int_{z=0}^{z=z_g} |k| dz \right] \quad (28)$$

where $k = (\mu_N^2 - m_N^2)^{1/2}$ is the wave number, and the chemical potentials are known from the numerical solutions. A few examples are shown in Fig. 7. Here we again choose $e\phi_e(R_S) = 30$ MeV and plot the dependence on density at zero temperature, and the dependence on temperature for the maximum density crust of each composition.

The integral in Eq. (28) can be approximated at $T = 0$ by

$$\log \tau \simeq -2\sqrt{2}m_N \int_0^{z_g} \left(\frac{Z}{m_N} e\phi_e(r) - \Delta\phi_g \right)^{1/2} dz \quad (29)$$

$$= -2\sqrt{2}CZ \int_{x(R_S)}^{x(R_C)} x^{-3} (x^2 - \Delta\phi_g)^{1/2} dx, \quad (30)$$

where

$$x = \left(\frac{Z}{m_N} e\phi_e(r) \right)^{1/2}, \quad (31)$$

using Eq. (1) for μ_N and Eq. (14) for $e\phi_e(r)$. Remem-

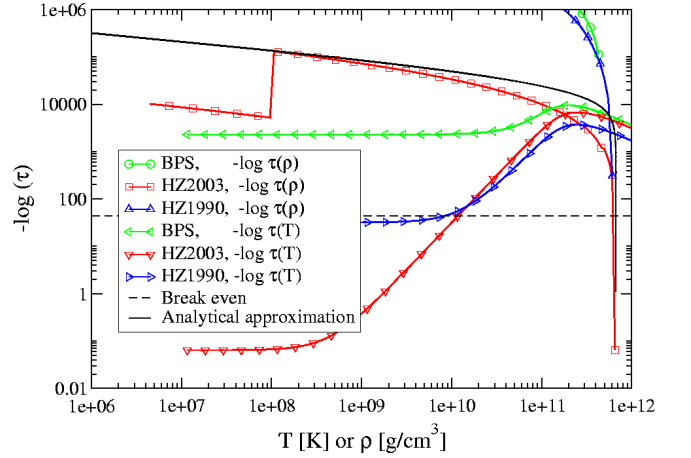


FIG. 7: Dependence of the transmission coefficient on density at $T = 0$, and on temperature at maximum density with $e\phi_e(R_S) = 30$ MeV. The kink in the HZ2003 density dependence is at the assumed transition to a hydrogen crust. The horizontal line marks the break even estimate for accreting stars in the text.

bering that $e\phi_e(R_C) = \frac{m_N}{Z} \Delta\phi_g$ this gives

$$\log(\tau) = -\frac{2\sqrt{2}CZ}{\Delta\phi_g^{1/2}} \left[\cos^{-1} \left(\frac{m_N \Delta\phi_g}{Ze\phi_e(R_S)} \right)^{1/2} - \left(\frac{1 - \frac{m_N \Delta\phi_g}{Ze\phi_e(R_S)}}{\frac{Ze\phi_e(R_S)}{m_N \Delta\phi_g}} \right)^{1/2} \right], \quad (32)$$

where $\Delta\phi_g$ can be approximated by Eq. (23). As seen from Fig. 7 Eq. (32) is a very reasonable approximation. Assuming the HZ2003 crust composition at drip density, the low density limit of Eq. (32) is given as

$$\log(\tau) \approx -2.5 \times 10^4 \left[\frac{\pi}{2} \left(\frac{\rho}{\rho_D} \right)^{-1/6} - 1.84 \right]. \quad (33)$$

The transmission coefficient may be better appreciated by estimating its value when transmission of ions into the core through the barrier breaks even with typical accretion rates in binary systems. That is, we require the balance:

$$\frac{\dot{M}}{m_N} \leq N_{ion} \times f \times \tau, \quad (34)$$

where \dot{M} is the mass accretion rate onto the strange star from a companion, N_{ion} is the number of ions, whose motion about their lattice position allows them to strike the barrier, and f is the oscillation frequency of this motion. N_{ion} may be taken as roughly the number of ions within one lattice distance, $a \sim 200$ fm, from the crust boundary, and following again Alcock et al. [4], the oscillation frequency should be less than 1 MeV. For a strange star

accreting $10^{-10}M_{\odot}\text{yr}^{-1}$ we then arrive at the condition

$$-\log \tau \geq 44.6 - \log \left(\frac{\dot{M}}{10^{-10}M_{\odot}\text{yr}^{-1}} \right) + \log \left(\frac{f}{\text{MeV}} \right) + \log \left(\frac{\rho}{4.3 \times 10^{11} \text{ g/cm}^3} \right) + \log \left(\frac{a}{200 \text{ fm}} \right) + 2 \log \left(\frac{R_S}{10 \text{ km}} \right) \quad (35)$$

as indicated in Fig. 7 (all logarithms are base e). It may then be noted that the maximum density models shown in Fig. 7 – except the one using the BPS chemical composition – will interact with the core at low temperature and are not stable at these densities. Only the BPS equation of state is thus able to remain stable at neutron drip density even with $e\phi_e(R_S) = 30$ MeV. For other compositions and lower $e\phi_e(R_S)$ stable crust densities are lower depending on the temperature, see Fig. 14.

VI. RESULTS FOR NON COLOR-FLAVOR LOCKED STRANGE STAR CORES

We have performed similar calculations for the case of non color-flavor locked cores (“ordinary” strange stars), and the structure of a solution with $\rho_{crust} = 4 \times 10^{11} \text{ g/cm}^3$, $T = 0$, $\mu_q^+ = 30$ MeV and the HZ2003 crust composition is shown in Figs. 8, 9, and 10. Charge neutrality is imposed at the starting point 1000 fm into the core and as we approach the surface electrons become scarcer and consequently the charge density and electric field rises. At the surface the quarks and their positive charge vanish, the charge density becomes negative and the field starts decreasing. The solution from the surface out looks like the color flavor-locked case with $e\phi_e(R_S) = \mu_e(R_S)$.

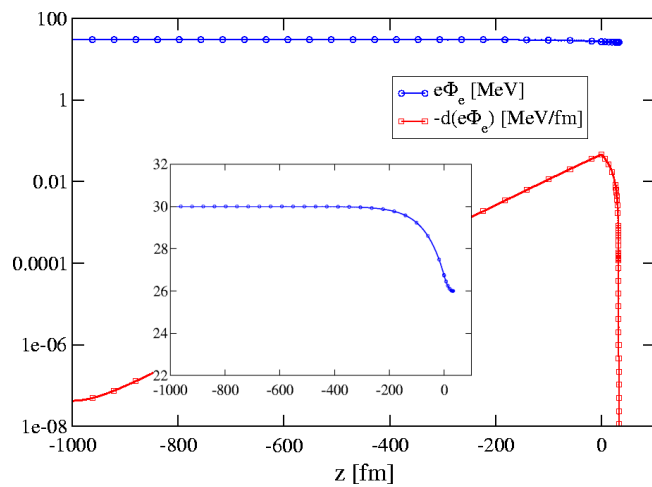


FIG. 8: Electric potential and field for a solution in the non color-flavor locked case. The inset focuses on the electrical potential.

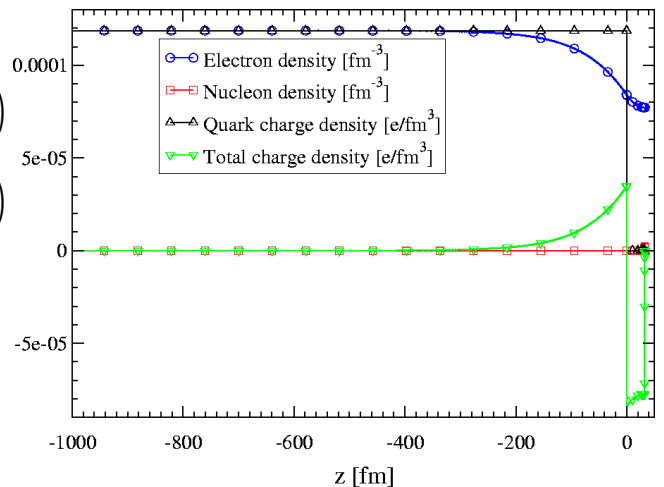


FIG. 9: Electron, nucleon, quark charge density and total charge density for the same solution as in Fig. 8. The transition to the crust is shown in Fig. 10.

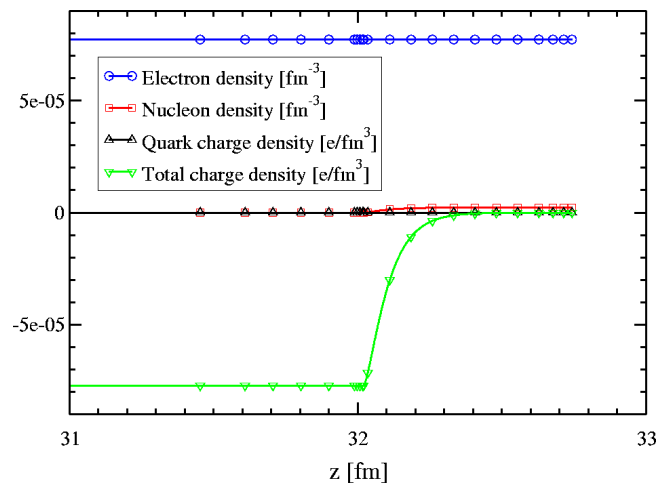


FIG. 10: Electron, nucleon, quark charge and total charge density during the transition from gap to crust for the same solution as in Figs. 8 and 9.

We again calculate the dependence of the gap width on density shown in Fig. 11 for $T = 0$ and different choices of $\mu_q^+ = 10, 20, 30, 40$ MeV from left to right. We only show models using the HZ2003 crust composition, since the gap width is in this case so insensitive to the choice of composition that the curves would be indistinguishable. Note again that only for the highest choice of $\mu_q^+ = 40$ MeV does the crust reach neutron drip density before the gap goes to zero. The gap width is approximated by Eq. (24) using $e\phi_e(R_S) = \mu_q^+ = 10$ MeV. For a bare strange star we would have $e\phi_e(R_S) = 3\mu_q^+/4$ [4], whereas for dense crusts $e\phi_e(R_S) \simeq \mu_q^+$, but since large gap widths are insensitive to $e\phi_e(R_S)$ we use $e\phi_e(R_S) = \mu_q^+$ in all analytical approximations.

The temperature dependence of the gap width is explored in Fig. 12 for the case of $\mu_q^+ = 30$ MeV with

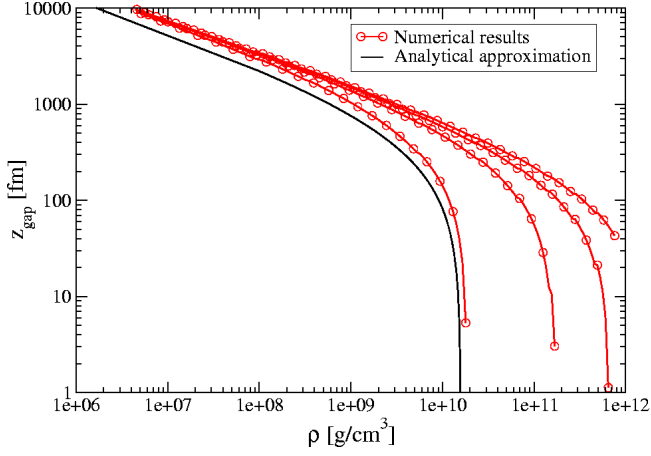


FIG. 11: Dependence of the gap width on density using the HZ2003 crust composition. From left to right $\mu_q^+ = 10, 20, 30, 40$ MeV. The analytical approximation explained in the text assumes $\mu_q^+ = 10$ MeV.

the HZ2003 crust composition. We note that the gap width declines steeply at $T \sim 10$ MeV and reaches zero at $T \sim 30$ MeV in contrast to the color-flavor locked case. This behavior is caused by the condition of charge neutrality at the starting point in the core (Eq. (27)), which reduces μ_e significantly at temperatures comparable to μ_q^+ . Other than that we note again the bump in the gap width caused by the condition of charge neutrality in the crust. The lowering of μ_e entirely suppresses the bump at high densities. The gap width is approximated in Fig. 12 by Eq. (13) using $e\phi_e(R_S) = \mu_e(z = -1000 \text{ fm})$ found from Eq. (27). $e\phi_e(R_C)$ is estimated as before from Eq. (8) and (25).

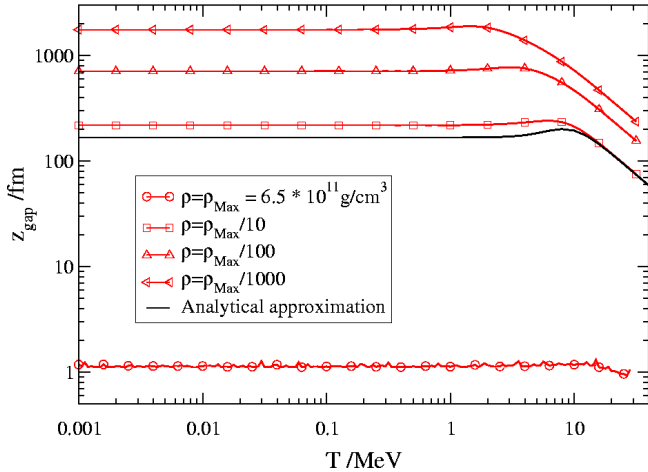


FIG. 12: Gap width dependence on temperature and density for non color-flavor locked cores with $\mu_q^+ = 30$ MeV. The maximum density is taken to be the density at which $z_{gap} \simeq 1$ fm as this is as close to zero gap width as is numerically reasonable – note that variations in the numerical results are significant only at this scale. The analytical estimate assumes $\rho = \rho_{max}/10$.

The variation of transmission coefficient with density and temperature is shown in Fig. 13. We again note that the bump is suppressed compared to the color-flavor locked case and that only crusts with the BPS composition can reach neutron drip before they become unstable against transmission through the Coulomb barrier.

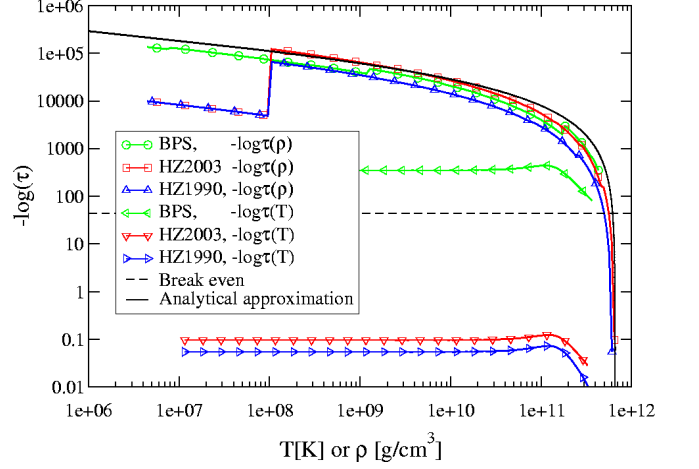


FIG. 13: Dependence of the transmission coefficient on density at zero temperature and temperature at maximum density for non color-flavor locked strange star cores with $\mu_q^+ = 30$ MeV. The kink in the HZ1990 and HZ2003 dependence corresponds to the assumed transition to a hydrogen crust. The break even estimate is explained in the text and the analytical approximation is based on Eq. (32) with the HZ2003 crust composition at drip density and $e\phi_e(R_S) = \mu_q^+$.

VII. DISCUSSION

We have expanded the treatment of gaps below strange star crusts to include effects of pressure and gravity on the crust nuclei and found the structure of the transition from gap to crust. Overall our results are as one would expect with a very sharp transition from gap to crust, gap widths ranging from a few fm at densities near neutron drip over a few thousand fm at densities close to the maximum to 10^{10} fm for very thin crusts. Crust densities are consequently limited below neutron drip unless one assumes an extreme Coulomb barrier height. If the gap width must be at least a crust lattice distance (~ 200 fm) and a reasonable value of $e\phi_e(R_S) \simeq 20$ MeV (or $e\phi_e(z = -1000 \text{ fm}) \simeq 20$ MeV) is assumed then the crust density is limited to a few times 10^{10} g/cm^3 .

The variation of the gap width with temperature is noteworthy in that it initially increases with temperature which is a qualitatively new feature. However this increase only takes place at temperatures below 1 MeV (10^{10} K) for crust densities which give very small gap widths of the order of 1 fm such as in the case of the HZ2003 crust at maximum density in Figs. 6 and 7. A realistic crust should have a sufficient gap width to be

stable against strong interaction with the core, and examples of such crusts could be the HZ1990 and BPS crusts in Figs. 6 and 7 – the HZ1990 crust is almost stable, and lowering the density a little to make it so would not change the dependence on temperature much. If we apply the criterion in Eq. (35) for crust stability we can find the highest stable density at given temperature and Coulomb barrier height, $e\phi_e(R_S)$. Numerical results for this are shown in Fig. 14 and we see that temperature effects are then not important below 10^{10} K. If we demand at least a crust lattice distance in non accreting systems the crust becomes even more stable against variations in the temperature.

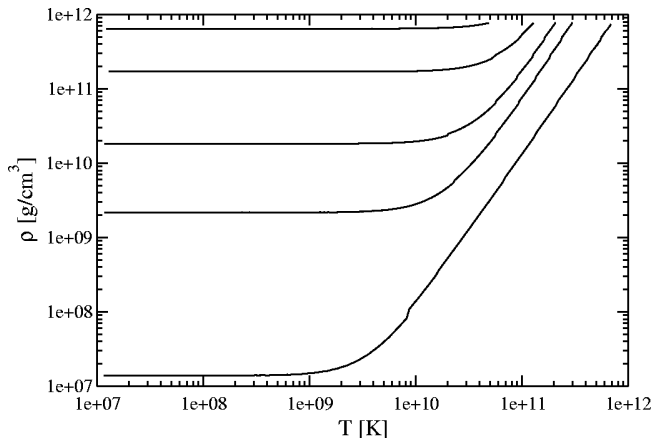


FIG. 14: Highest stable density according to Eq. (35) at given temperature and $e\phi_e(R_S) = 1, 5, 10, 20, 30$ MeV from below. The crust composition is from HZ2003 and we stop at the temperature corresponding to neutron drip density.

The thermal structure of accreting strange stars was investigated by Miralda-Escudé et al. [24] who found temperatures around 10^7 K at the crust boundary for strange stars accreting 10^{-11} to $10^{-9.83} M_\odot \text{ yr}^{-1}$ assuming that 10 MeV is released per nucleon converted to strange quark matter (bag constant $B = 103 \text{ MeV/fm}^3$). In this case the gap width would not be affected at all, and one might as well use the zero temperature results. Superbursters however are known to have much higher accretion rates around 0.1-0.3 times the Eddington accretion rate, $M_{\text{Edd}} \sim 10^{-8} M_\odot \text{ yr}^{-1}$, and in a recent investigation Page and Cumming [26] found temperatures for such stars in the range $10^8 - 10^9$ K at the crust boundary. This work was motivated by the difficulties in achieving carbon ignition at observed column depths in superburst models on neutron stars – see Cumming et al. 2005 [25] for a recent review – and it was found that superbursts may ignite at the right column density on strange stars provided that neutrino emission in the core is slower

than direct Urca which implies that strange quark matter should be a color superconductor. During the superburst itself temperatures in the range $2 - 7 \times 10^9$ K are reached for a few hours [23, 27]. This is again too low for significant temperature effects and for stable crusts one may as well use the zero temperature expressions.

The present treatment could be improved by including general relativity instead of Newtonian gravity, and by using a less simplistic model for the equation of state for the crust. Such improvements are necessary to calculate the properties of the whole star, but we expect the changes in the gap properties to be minor compared to the results presented here. The same can be said about a more detailed treatment of the quark phase, which has here merely been treated as a source of a given total mass and starting value for the electron chemical potential. However, as pointed out in [16], the electric potential in the outer layers of the strange core could be qualitatively different from the behavior assumed here if a mixed phase of quark nuggets and electrons can be realized.

Another important oversimplification involves the assumption of a constant pairing gap all the way to the quark core surface in the treatment of quark matter in the CFL-phase. In fact the pairing gap Δ_{CFL} may be envisaged to vanish within a surface distance of order $1/\Delta_{\text{CFL}} \approx 2-20$ fm for gap energies between 100 and 10 MeV. Possibly a range of phases appear in the extreme uppermost layers, including the possibility that the very surface resembles the ungapped ordinary quark phase also discussed above. A detailed treatment of gapped phases near a surface remains to be performed.

In conclusion the results of our expanded treatment, while quantitatively somewhat different, are qualitatively consistent with previous work in the literature with regards to gap width, transmission coefficient and possible crust densities. The increase in gap width with temperature is new but significant only at very high temperatures not likely realized. Perhaps the most useful results of the investigation are the various analytical approximations which have been derived and shown to fit the full numerical solutions very well, since these provide better physical insight and can be easily used in models for strange star rotation, glitches, accretion and instabilities.

Acknowledgments

This work was supported by the Danish Natural Science Research Council. We thank Fridolin Weber for useful comments on an early draft.

[1] G. Baym and S. A. Chin, Phys. Lett. B **62**, 241 (1976).

[2] E. Witten, Phys. Rev. D **30**, 272 (1984).

- [3] P. Haensel, J. L. Zdunik and R. Schaeffer, *Astron. Astrophys.* **160**, 121 (1986).
- [4] C. Alcock, E. Farhi and A. Olinto, *Astrophys. J.* **310**, 261 (1986).
- [5] J. Madsen, *Lect. Notes Phys.* **516**, 162 (1999) [arXiv:astro-ph/9809032].
- [6] F. Weber, *Prog. Part. Nucl. Phys.* **54**, 193 (2005) [arXiv:astro-ph/0407155].
- [7] K. Rajagopal and F. Wilczek, *Phys. Rev. Lett.* **86**, 3492 (2001) [arXiv:hep-ph/0012039].
- [8] J. Madsen, *Phys. Rev. Lett.* **85**, 4687 (2000) [arXiv:hep-ph/0008217].
- [9] J. Madsen, *Phys. Rev. Lett.* **87**, 172003 (2001) [arXiv:hep-ph/0108036].
- [10] V. V. Usov, *Phys. Rev. D* **70**, 067301 (2004) [arXiv:astro-ph/0408217].
- [11] C. Kettner, F. Weber, M. K. Weigel and N. K. Glendenning, *Phys. Rev. D* **51**, 1440 (1995).
- [12] Y. F. Huang and T. Lu, *Astron. Astrophys.* **325**, 189 (1997).
- [13] R. X. Xu and G. J. Qiao, *Chin. Phys. Lett.* **16**, 778 (1999) [arXiv:astro-ph/9908176].
- [14] K. S. Cheng and T. Harko, *Astrophys. J.* **596**, 451 (2003) [arXiv:astro-ph/0306482].
- [15] V. V. Usov, T. Harko and K. S. Cheng, *Astrophys. J.* **620** 915 (2005) [arXiv:astro-ph/0410682].
- [16] P. Jaikumar, S. Reddy and A. W. Steiner, preprint (2005) [arXiv:nucl-th/0507055].
- [17] J. L. Zdunik, *Astron. Astrophys.* **394**, 641 (2002) [arXiv:astro-ph/0208334].
- [18] H. Fu and Y. F. Huang, *Chin. J. Astron. Astrophys.* **3**, 535 (2003) [arXiv:astro-ph/0306259].
- [19] G. Baym, C. Pethick, P. Sutherland, *Astrophys. J.*, **170**, 299 (1971)
- [20] P. Haensel and J. L. Zdunik, *Astron. Astrophys.* **229**, 117 (1990).
- [21] H. Schatz, A. Aprahamian, V. Barnard et al., *Phys. Rev. Lett.* **86**, 3471 (2001) [arXiv:astro-ph/0102418].
- [22] P. Haensel and J. L. Zdunik, *Astron. Astrophys.* **404**, L33 (2003). [arXiv:astro-ph/0305220].
- [23] H. Schatz, L. Bildsten, A. Cumming, *Astrophys. J.* **583**, L87 (2003)
- [24] J. Miralda-Escudé, P. Haensel, and B. Paczynski, *Astrophys. J.* **362**, 572 (1990)
- [25] A. Cumming, J. Macbeth, J. J. M. in't Zand and D. Page, preprint (2005) [arXiv:astro-ph/0508432].
- [26] D. Page, A. Cumming, preprint (2005) [arXiv:astro-ph/0508444].
- [27] A. Cumming, L. Bildsten *Astrophys. J.* **559**, L127 (2001)